In: AIAA SciTech Forum 2023, 23-27 January 2023, National Harbor, Maryland, USA
DOI:10.2514/6.2023-1733

Unmanned Aerial System Concept Design for Rail Yard Monitoring

Alain Kirenga*, Hae-In Lee†, Argyrios Zolotas‡
Centre for Autonomous and Cyber-Physical Systems, SATM, Cranfield University, MK43 0AL, UK

Safety and security monitoring in large yard areas, typical in rail yard environments, is an important task and any trespassing or vandalizing incidents can cause significant disruptions to routine activities and possibly to staff safety. This can impact normal rail network operation. This paper investigates the feasibility of using low-cost unmanned aerial systems (UAS) for monitoring rail yards. A rigorous literature survey on unmanned aerial vehicles (UAV) platforms for monitoring in various sectors is conducted. Given the large area of the rail yard, a concept of multiple rotor-based UAVs is explored with a particular eye on energy-efficiency. The proposed concept is validated hardware-wise through multiple flights conducted to monitor a scale-down setup of a "yard" concept in the lab's indoor flying arena. Analysis of the results showcases the potential of using low-cost multirotor UAV solutions for monitoring assistance in large yards.

I. Introduction

Rail yards are an integral and critical part of the rail network. Routine activities at a rail yard include assembling/disassembling of train vehicles, inspection/maintenance and storage of rail vehicles [1]. Given the size of the train assets and the required storage and activity area, rail yards tend to be large areas/ sites and this poses challenges in terms of monitoring safety and security. Actually illegal trespassing and vandalism of critical assets inside rail yards can cause major disruptions of services, which poses not only dangerous situation for the safety of staff but can also be very costly to the rail network and operators [2, 3]. Due to the large area of the yards, physical security monitoring with traditional methods using CCTV surveillance systems and human patrols is cost prohibitive and rather inefficient (for example CCTV is subject to blind spots) [4].

With recent advances in Unmanned Aerial Vehicles (UAVs) technology, medium to smaller scale UAV platforms equipped with vision sensors provide a potential solution to performing the monitoring/surveillance tasks at a higher frequency which can improve the yard's security. Moreover, UAV platforms can respond faster in case of an identified security incidence for preview information.

This paper presents a low-cost UAV concept design for rail yard security monitoring by investigating UAV platforms and systems used for monitoring in various sectors. In particular, a concept is developed focusing on the endurance of the multi-rotor UAVs. A practical methodology to design energy-efficient UAV platforms is proposed with appropriate selection of the propulsion system and other components to meet system requirements. Additionally, a state-of-the-art object detection algorithm is implemented in an onboard computer to assess its overall performance during the monitoring task. The proposed concept is validated by following a scaled-down indoor lab setup of a "rail yard monitoring area" using the custom-built UAV platform.

II. Work in the literature on monitoring using UAV platforms

Considering the terrain characteristics of a rail yard, this paper analyses UAV systems used to monitor in almost similar applications such as railway network, civil infrastructure, crowd monitoring, forest fires and oil pipelines. Flammini et al. [5] survey drone technology and its use for automated surveillance of railways. The authors use small multirotor UAV equipped with onboard computer and camera to perform the surveillance. The authors do not provide a comprehensive concept that employs UAVs to automatically monitor railway infrastructure. They rather focus on the UAV system engineering and discuss issues related to computer vision algorithms. A similar paper of Flammini et al. [6] proposes a concept of using a UAV-based surveillance system capable of performing monitoring of railway infrastructure systems and suitable for applications such as structural monitoring and physical security monitoring. The

*MSc Autonomous Vehicle Dynamics and Control Student, SATM.
†Lecturer in Autonomous Systems and AI, SATM.
‡Reader in Systems and Control, SATM.

proposed system uses multirotor UAV as agents to collect data and send them through a network infrastructure. Unlike this paper, the work in [6] does not implement any hardware or software simulations to validate the proposed concept. Both works [5, 6] use multirotor UAV systems to conduct monitoring tasks.

In [7], the authors demonstrate an inexpensive and easy-to-operate fixed wing UAS equipped with multispectral sensor that captures imagery data for infrastructure assessment tasks on large areas such as oil pipeline and railways. Endurance-wise, the fixed wing vehicle can fly up to 60 mins. Authors in [8] presented a flexible launch and landing fixed-wing UAV with hyperspatial image resolution to demonstrate procedures of monitoring of abandoned dreg fields of railway. The fixed-wing UAV is suitable for monitoring large areas; however, the infrastructure requirements pose a barrier for its deployment in an area such as a rail yard with no open fields. Rotary wing UAV solutions are deemed a more practical choice in closer spaces.

To address the limitations of a single small multirotor UAV in terms of its effectiveness in monitoring tasks, the works in [9, 10] propose a perimeter surveillance based on multiple UAVs. Through simulation validation and results, the authors demonstrate that the use of multiple UAVs increases system's reliability and efficiency. However, the single multirotor UAV unit suffers from limited endurance. To tackle the problem of using energy-constrained rotary-wing platforms for monitoring purposes, different solutions have been proposed in the literature. One approach is using tethered multi-rotor UAVs as proposed in [11] whereby the authors develop a photovoltaic power management system to enhance the endurance of a swarm of multiple tethered multirotor UAVs. The disadvantage of tethered multirotor UAVs is the restricted freedom of movement and area of operation. An alternative solution is using static charging stations to increase UAV endurance as proposed in [12, 13].

The deployment of a single multirotor UAV for monitoring a large area such as a rail yards, while the ideal solution, is challenging given the mission requirements. A team of multiple multirotor UAVs with designated areas for monitoring is a more viable solution for monitoring a large rail yard. This paper presents a concept which uses a team of multirotor UAVs to conduct rail yard surveillance for detection and deterrence of potential trespassers and intruders.

III. Concept Development

The system's requirement is to be able to detect and track trespassers inside a rail yard. The system must have a sensor for detection and a reliable communication link. Using multiple multi-rotor UAVs is deemed a more feasible solution since multirotor UAVs have VTOL and hovering capabilities. They are flexible and can take-off mostly anywhere inside a rail yard as they do not require sophisticated launch and recovery systems. To address the issue of endurance for individual UAV agents, the concept proposes recharging stations to be mounted on top of depot building to reduce the probability of them being tampered with. Figure 1 demonstrates the proposed concept with multiple UAVs conducting a monitoring mission to ensure the security of the rail yard.

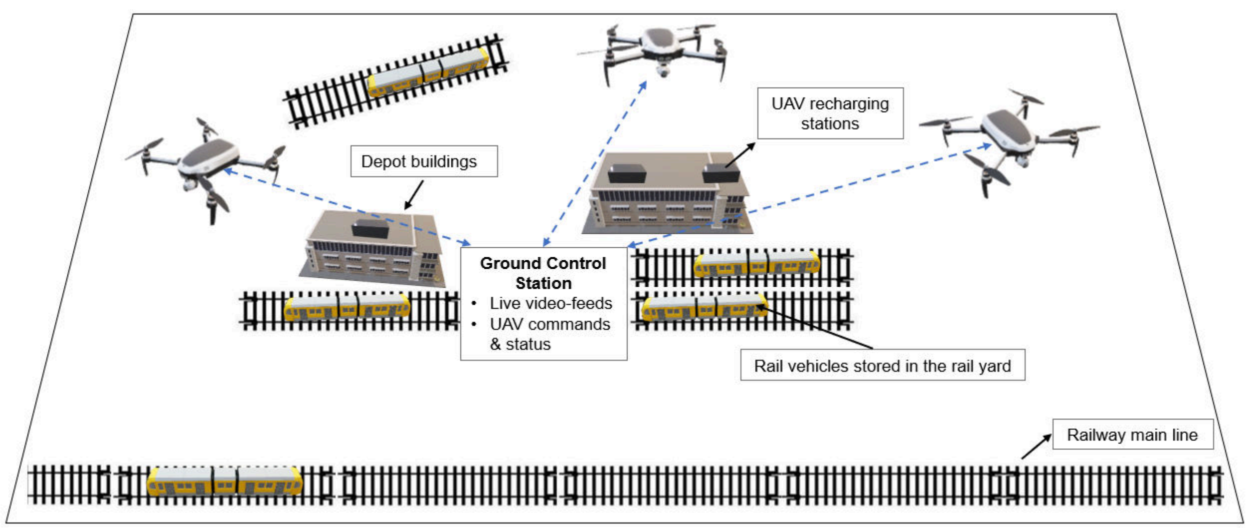

Fig. 1 Conceptualisation: rail yard security with UAVs.

IV. UAV System Development

This section develops a UAV unit and, in particular, conducts endurance analysis. A way to improve UAV endurance is to design energy-efficient platforms [14]. Here a small quadcopter unit with a maximum take-off weight (MTOW) of 2 kg is considered, and the components of the UAV are selected so that the vehicle thrust-to-weight ratio is equal to 2 during hover. Concerning the multirotor UAV design, the work in [15] proposes a UAV design flow using an iterative process to find the MTOW; however, it does not provide details on the selection of individual UAV components. The work in [16] proposes a UAV design methodology which accounts for the selection of UAV components. However, the above-mentioned works do not account for MTOW constraint. In this paper, we extend the work and utilise a combination of the design methodologies described in [15, 16] with MTOW constraint.

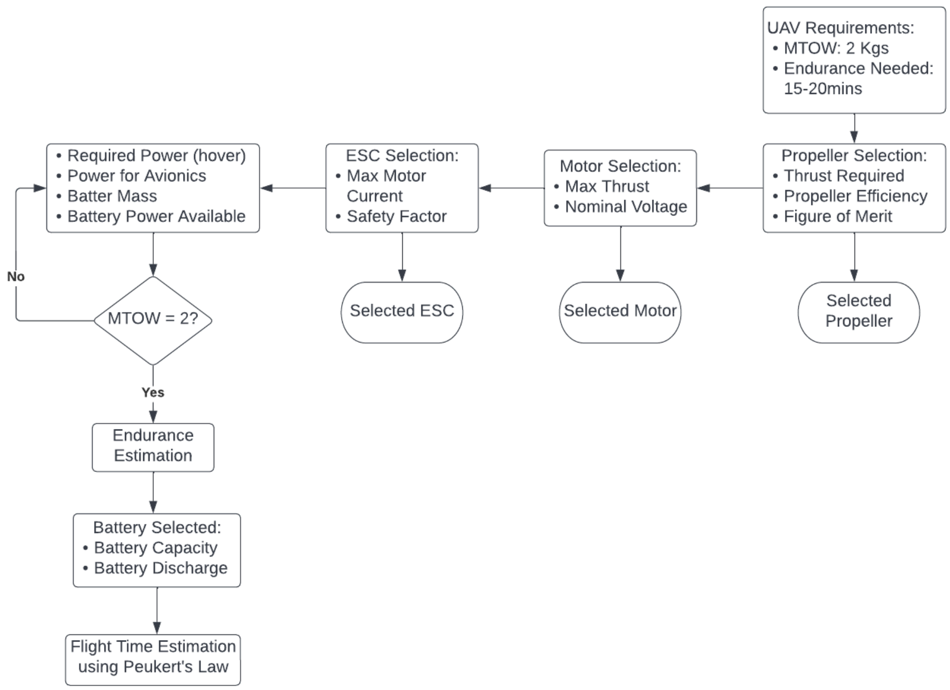

Fig. 2 Design Flow Chart.

Figure 2 shows the system design flow, i.e. from the set of requirements, through the individual components selection with a focus on the efficiency of the components. A *Peukert's battery model* which assumes constant power draw is used to determine the UAV flight endurance.

A. Propulsion System

The propulsion system is composed of the propellers, motors, electronic speed controllers (ESC) and battery. Appropriate selection of the propulsion system ensures an efficient platform, supporting maximum flight endurance. A carbon fiber frame (s500) is used for the quadcopter UAV. The size of the frame limits the size of the propeller one can use. A thrust stand is used to evaluate the efficiency of two propellers with different dimensions as shown in Figure 3. Both propellers have the same pitch (4.5 in), but different diameters (10 in and 11 in). To select the most efficient propeller, the thrust and the mechanical power need to be known. Using the results plotted in Figure 4, the 11-inch propeller bears the highest thrust to mechanical power ratio (N/W) at the required thrust for hover based on the MTOW, and is therefore selected. Given that the selected propeller has a relatively long diameter, a motor with low motor velocity constant (850 kv) is proposed [14]. Based on the thrust test, the maximum current draw of one motor is 17A. Hence, an ESC capable of supplying 25A continuously is chosen to account for a safety margin.

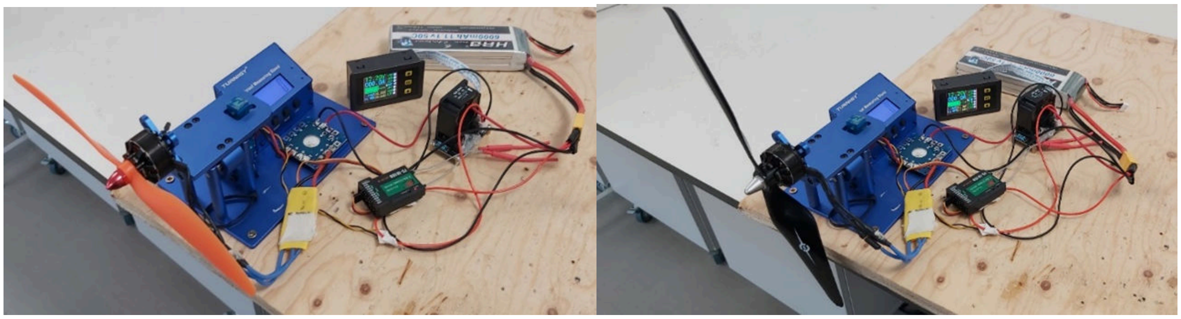

(a) 10x4.5in Propeller. (b) 11x4.5in Propeller.

Fig. 3 Thrust performance test of two propellers.

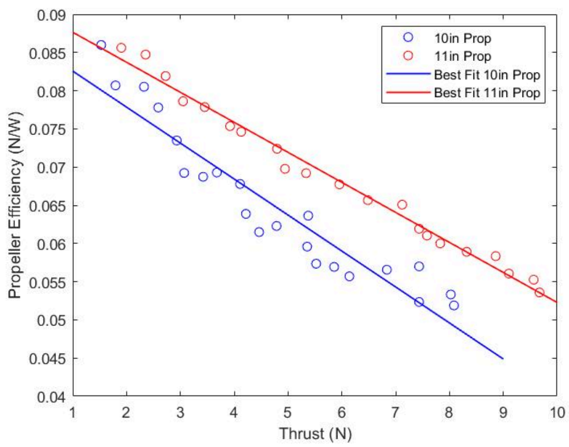

Fig. 4 Propeller Efficiency vs Thrust.

B. Image Processing Equipment

The state-of-the-art object detection algorithm such as You Only Look Once (YOLO) requires significant computation power to run in real-time. Onboard computers are usually low-powered devices with limited computation power. This works utilises an NVIDIA Jetson Nano Developer kit, a popular platform widely used as an onboard computer designed specifically for deep learning applications. The Jetson Nano DK has a 1.43GHz processor with 4GB memory and a 128-core Maxwell GPU [17]. The onboard computer weight is 141 grams and it can consume up to 15W at maximum power draw. A 2-megapixels wide angle USB camera is used to provide images to the onboard computer. To enhance image stability, a three-axis gimbal, Tarot T-3D IV, is used given its small footprint.

Considering that the total take-off weight W_{T_o} of the electric multirotor UAV is expressed as [15]:

$$W_{T_o} = W_o + W_b + W_{p_l}, \tag{1}$$

where W_o is the zero-battery weight including the frame, the avionics, and the propulsion system, W_{p_l} is the payload weight including the onboard computer, the gimbal and the camera, and W_b is the battery weight. The total mass of the UAV without the battery is an important parameter when sizing the battery W_b.

C. Battery/ Energy Storage

LiPo battery is mostly used in small UAVs given its high energy density and high current discharge capabilities [16]. The battery comprises a high percentage of the weight of the UAV and the correct selection of the battery will substantially impact flight time. The targeted flight time for the quadcopter platform is between 15 – 20 mins at 80% battery depth of discharge. The endurance of the UAV can be estimated using the battery energy and the power required for the UAV to hover:

$$E = \frac{E_b}{P_{h_e}}, \tag{2}$$

where E_b denotes the battery energy expressed in W h, and P_{h_e} is the electrical power required for the UAV to hover. E_b can also be expressed in terms of the battery specific energy as:

$$E_b = E_{spec} \cdot m_b \cdot n_b \cdot f_{DOD}, \tag{3}$$

where E_{spec} is the battery specific energy expressed in W h/kg and can range between 50.7 – 220 W h/kg for LiPo batteries [15], m_b is the mass of the battery, n_b is the battery efficiency accounting for heat losses, and f_{DOD} is the battery depth of discharge [15]. It is recommended not to discharge batteries beyond 80% depth of discharge to ensure a longer battery life [16].

The power required at hover P_{h_e} is obtained using momentum-theory [18] and computed as below assuming a 90% motor efficiency:

$$P_{h_e} = \left(\frac{W_{T_o}^{3/2}}{f \cdot \sqrt{2 \cdot \rho \cdot \pi \cdot N_r \cdot r_{prop}}} \right) /0.9, \tag{4}$$

where N_r is the number of rotors with radius r_{prop}, ρ is the air density and f is the figure of merit which is typically between 0.5 and 0.7 [18]. A value of $f = 0.5$ is used in this paper.

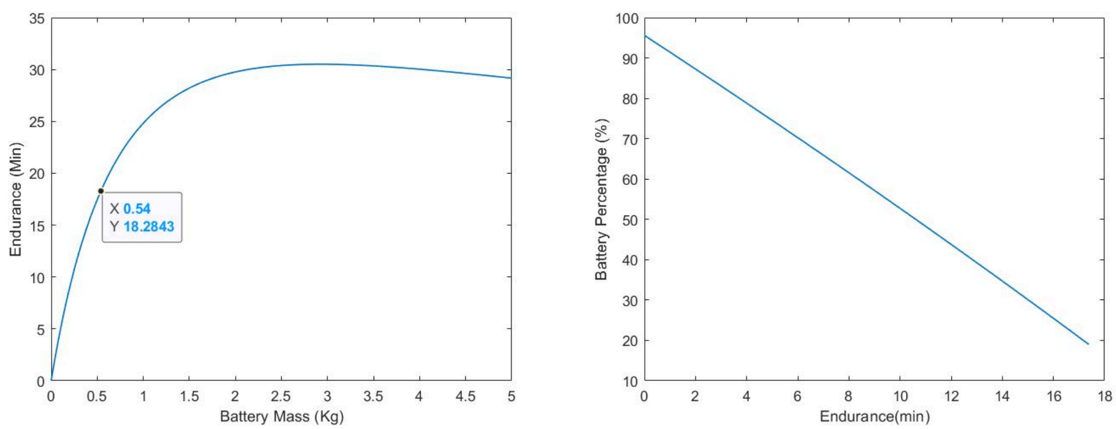

(a) UAV endurance as a function of battery mass.

(b) Peukert's Battery Discharge Model.

Fig. 5 Endurance related responses (battery)

Using manufacturer's data and actual measurements, the mass of the UAV without the battery is found to be 1.41 kg. Assuming an E_{spec} = 185 W h/kg and n_b = 95%, a battery mass of greater than 0.4 kg is required to ensure an endurance of at least 15 mins using Eq. (2). To maximise the UAV endurance under a MTOW constraint, a battery mass of 0.54 kg is required as depicted in Figure 5a. Using the above preliminary results, a 3S battery with 8500mAh capacity weighting 0.525 kg is selected for the UAV.

To estimate accurately the endurance of the UAV, a Peukert's model which assumes a constant battery discharge is used following the process described in [16, 19]. A Peukert's constant of 1.05 for LiPo batteries is adopted as suggested in [19]. As shown in Figure 5b, the estimated endurance for the UAV using the proposed battery model is 17.38 mins with 20% remaining battery capacity.

V. Hardware and Experimental Setup

A. Hardware Architecture

The block diagram of the UAV platform with the selected components is shown in Figure 6. The UAV flight controller is a Pixhawk 5X running ArduPilot which is a widely used open-source autopilot. The autopilot is responsible for the low-level control of the UAV. Through a telemetry radio, the status of the UAV such as position, speed, battery health and other embedded FC sensors are transmitted to the Ground Control Station (GCS), and simultaneously, the GCS can send commands such as flight mode changes and attitude commands. The NVIDIA Jetson Nano onboard computer runs the object detection algorithms on images received from the gimbal mounted camera. The complete multirotor UAV designed and built for validation tests is shown in Figure 7.

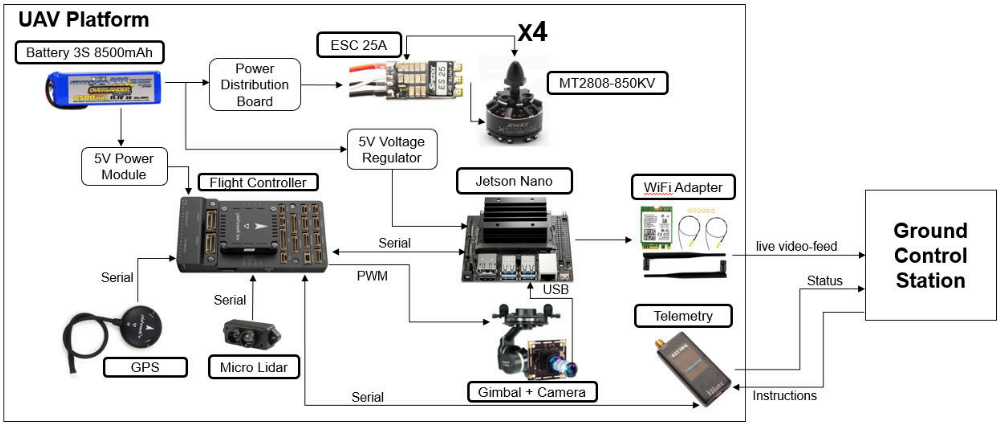

Fig. 6 UAV platform block diagram.

Fig. 7 Multirotor UAV.

B. Experimental Setup

To validate the proposed concept and design methodology, a small-scale "rail yard" is implemented inside an L-Shaped indoor flying arena with a length of 16.5 m on the longest side, width of 20 m and a height of 4 m. Three main structures found inside rail yards namely rail vehicles, depot building and "objects" to detect are constructed on a smaller scale. Regarding the "objects" to detect, it was decided to use "sport balls" in lieu of persons given their smaller dimensions and for safety purpose.

Before each flight, pre-flight checks are conducted, and the battery pack is checked to ensure that it is fully charged. VICON motion capture system is used to record the flights for post-flight analysis. Using the Mission Planner software, flight logs are also extracted for post-flight analysis.

VI. Results and Analysis

This section presents the results of the endurance tests under various conditions to validate the proposed design methodology. In particular, the flight tests examine the impact of a hover flight, a forward flight, and the impact of running onboard an object detection algorithm. These conditions are chosen to reflect the conditions faced by a multirotor UAV during a monitoring mission. Furthermore, this section details the results of the performance of the object detection algorithm under light and dark conditions.

A. Hover Flights with Various Payload Weight

For monitoring tasks, UAVs equipped with a gimbal mounted camera spend considerable amount of time in a hovering state to detect and track objects of interests. To assess the impact of weight on the endurance of the UAV, flights were conducted at a take-off weight of 2 kg and 2.1 kg. For consistency, the onboard computer which consumes the most avionics power was switched on to run the object detection algorithm.

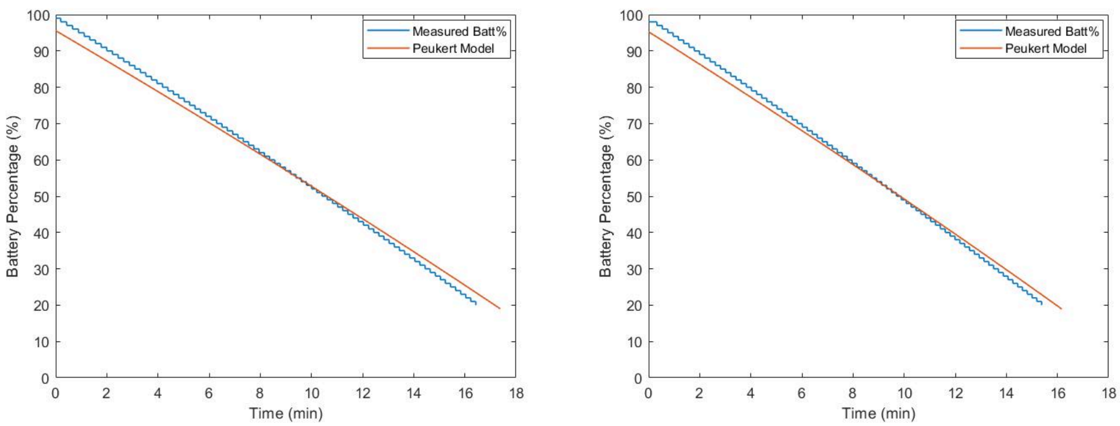

(a) MTOW: 2.0 kg.

(b) MTOW: 2.1 kg.

Fig. 8 Endurance flight test results in hover condition

Table 1 Hover Flights Results

MTOW (kg)	Endurance (min)			Error (%)
	E_{Est} (Peukert)	E_{Meas} (mean)	E_{Meas} (std)	
2.0	17.38	16.52	0.095	5.21%
2.1	16.17	15.26	0.115	5.96%

Three flights were conducted at a take-off weight of 2 kg while two flights were performed at 2.1 kg take-off weight. The statistics of the endurance flight tests in terms of mean value and standard deviation are provided in Table 1. The difference between the estimated endurance using Peukert's battery model and the flight time gives an error of 5.21% and 5.96% for the take-off weight of 2 kg and 2.1 kg respectively. The error is significantly low which suggests that the proposed battery model is adequate to accurately estimate the endurance of the multirotor UAV in hover condition.

Figure 8 shows the results of the endurance flight tests conducted at MTOW of 2.0 kg and 2.1 kg respectively. The test results demonstrate that the endurance is reduced by almost one and a half min with an additional 100 g payload weight. The results show that the weight is a major factor on the endurance of the multirotor UAV. Therefore, the proposed hardware-optimization approach of selecting UAV components with less weight and more efficiency leads to an energy-efficient UAV.

B. Forward Flights

To assess the impact of conducting a monitoring task on the UAV endurance, a search pattern was designed and executed inside the indoor flying arena.

Four flights were conducted to assess the endurance of the UAV while executing a monitoring mission. The endurance test result in a forward flight is depicted in Figure 9b, while the UAV for the result shown in Figure 9a travelled at 0.5m/s. Note that no flight test exceeded 3 m/s for safety given the restricted size of the flying arena. As

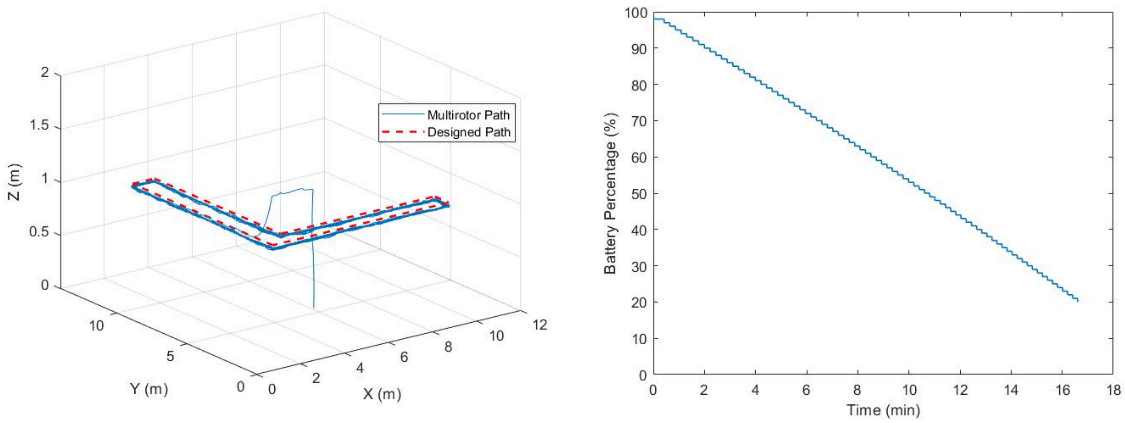

(a) Search Pattern Flight Test.

(b) Endurance flight results for a forward flight.

Fig. 9 Endurance: Search pattern and endurance flight response (fwd flight)

Table 2 Forward Flights Results

MTOW (kg)	Hover Flight Endurance (min)		Forward Flight Endurance (min)	
	E_{Meas} (mean)	E_{Meas} (std)	E_{Meas} (mean)	E_{Meas} (std)
2.0	16.52	0.095	16.61	0.105

presented in Table 2, a comparison of the results of the hover and the forward flights shows a difference of only six seconds in endurance. Despite the benefits of the controlled indoor environment, the small-scale rail yard setup in the flying arena constrains the UAV speed. The slightly higher flight time observed in the forward flights can be attributed to the reduction of the induced propeller drag during forward flights [16, 18].

C. Impact of Avionics Power Consumption

The battery provides the electrical power to the motors as well as to the avionics components which include the flight controller, the onboard computer, the gimbal, and other peripherals. Table 3 shows the power consumption measurements of the different avionics components obtained using the power module attached to the flight controller.

Table 3 Avionics Power Consumption

Components	**Voltage**(V)	**Current**(A)	**Power**(W)
Flight Controller	5	0.426	2.13
Gimbal + Other Peripherals	12	0.18	2.12
Jetson Nano without YOLOv5	5	0.55	2.75
Jetson Nano with YOLOv5	5	2.4	12
Total Power without YOLOv5			7
Total Power with YOLOv5			16.25

As shown in Table 3, deploying the object detection algorithm YOLOv5 inside the Jetson Nano required 12 W, hence making the onboard computer the highest avionics power consuming device. To assess the impact of running YOLOv5 algorithm on the endurance of the UAV, four hover flights were conducted at MTOW of 2 kg without the object detection algorithm.

As illustrated in Figure 10, the overall power draw is increased throughout the flight when the YOLOv5 algorithm is running onboard. Hence, as shown in Table 4, implementing YOLOv5 in an onboard computer to detect potential

Table 4 Impact of Object Detection Algorithm on UAV endurance

MTOW(Kg)	Hover Flight with YOLOv5(min)		Hover Flight without YOLOv5(min)	
	E_{Meas} (mean)	E_{Meas} (std)	E_{Meas} (mean)	E_{Meas} (std)
2.0	16.52	0.095	17.33	1.024

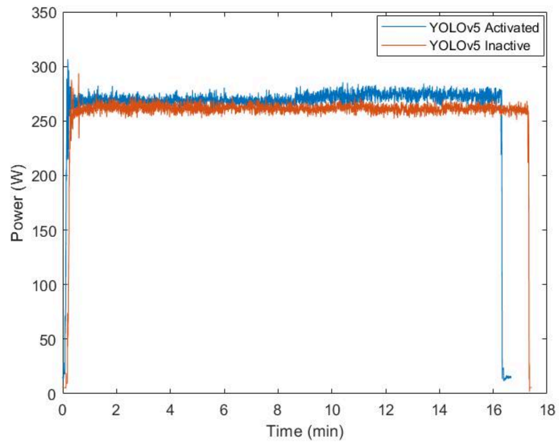

Fig. 10 Impact of running YOLOv5 on Power Consumption.

trespassers reduces the UAV endurance by almost a minute. This time is negligible compared to the benefits of the state-of-the art computer vision algorithm; however, it must be factored in the overall operation of the system.

D. Object Detection Algorithm Results

To speed up the analysis of images taken from the gimbal mounted camera on the UAV, this paper proposes to leverage the open-source YOLOv5 detector. By doing so, time consuming tasks of manually detecting and identifying trespassers in images can be replaced with trained object detectors based on deep neural networks. Here, the performance of the YOLOv5 is assessed in terms of speed and accuracy. The object detection algorithm is implemented in the Jetson Nano to detect "sports balls" which is a class that is part of the open-source COCO dataset. Frames per Second (FPS) metric is used to evaluate the speed of the algorithm. By enabling CUDA, the Jetson Nano was able to successfully achieve 7.3 FPS. The achieved speed performance allows real-time application such as visual-based navigation. To further assess the performance of the algorithm, real-flight tests were conducted inside the small-scale rail yard under different lighting conditions. The UAV was flown to detect sports ball with the lights on and off in the flying arena.

The algorithm outputs a confidence score that represents a measure of how confident the algorithm thinks the object is present in the frame. The default confidence threshold parameter was increased from 0.25 to 0.5 at the beginning of the flight tests.

(a) Ball without nearby objects (lighter condition).

(b) Ball near one "rail vehicle" (lighter condition).

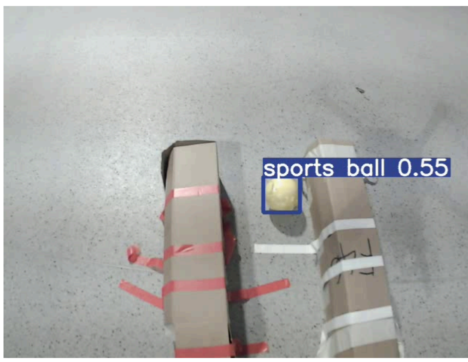

(c) Ball in between two "rail vehicles" (lighter condition).

(d) False positive detection (lighter condition).


(e) No sports ball detected (darker condition).

(f) No sports ball detected (darker condition).

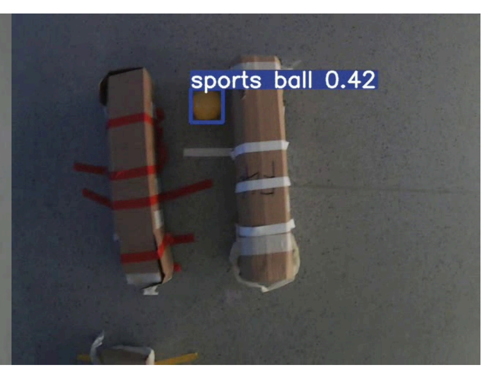

(g) Sports ball detected (darker condition).

(h) Sports ball detected (darker condition).

Fig. 11 YOLOv5 performance in light and dark environment.

With a confidence threshold of 0.5, YOLOv5 algorithm can detect with the highest confidence score the ball placed without any objects nearby in Figure 11a. The algorithm manages to detect the sports balls placed near the "rail vehicle", but at a much lower confidence score, especially when the ball is placed between two "rail vehicles". Furthermore, false-positives detection of small yellow tapes placed in the flying arena were detected as sports ball. Despite not having a custom dataset dedicated to "sports balls", YOLOv5 trained on the COCO dataset achieves a confidence level between 50 to 90% when detecting the sports balls in good lighting conditions.

In a dark lighting environment, the algorithm showed poor detection performance. The algorithm struggled to detect properly the objects of interest with the same confidence threshold. Hence, the confidence threshold was lowered from 0.5 to 0.4. The algorithm failed to recognize the "sports ball" placed in the dark side of the flying area as evidenced in Figure 11e. Post-analysis of the images frames indicates that there was only one instance where the algorithm was able to detect the sports ball placed between the two "rail vehicles" as shown in Figure 11h. In this case, the detection confidence score was very low at 42%. In contrast, the algorithm detected with ease the sports ball which was placed near the lighting source from the window of the flying arena. Here, the confidence level ranged from 43 – 75% as shown in Figure 11g. The lighting source from the window proved to be a major factor for the performance of the algorithm in a dark environment.

A dedicated dataset, including objects of interests in different lighting conditions, would provide better results with a higher confidence level. Furthermore, with a customised dataset trained on YOLOv5, the performance of the algorithm would be evaluated qualitatively using metrics such as the mean average precision, F1 score and intersection over union of the boundary boxes, instead of only relying on the confidence score from inference data.

VII. Conclusion

This paper presents the development of a low-cost UAS concept for rail yard monitoring. The hovering and VTOL capabilities of the multi-rotors are suitable for a rail yard given the ground features and monitoring requirements. A multirotor UAV is designed with particular focus on the endurance, following appropriate selection of energy-efficient components as key to maximising flight time. The flight test results show that the battery model provides accurate endurance estimation with only 5.2% deviation. Additionally, the obtained results confirm the feasibility of using YOLOv5 onboard for outliers, in this scaled-down scenario being "sports balls", detection. With a 7.3 FPS speed, YOLOv5 running on the Jetson Nano demonstrates real-time application capability. The algorithm also shows adequate performance in a good lighting condition; however, it performs poorly in a darker lighting conditions environment. In the next stage improvements will be looked at in terms of training the object detection algorithm on a customised dataset in different lighting conditions as well as implementing a tracking algorithm to track moving features in a large yard. This work concentrated on the single multirotor UAV, with functionalities of multiple UAVs to explore in the work sequence. The work sets the baseline of such a working concept, with future outdoor flight tests outdoors forming more realistic validation.

Acknowledgments

The work stems from an MSc Autonomous Vehicle Dynamics and Control project outcome. The author thanks the project reviewers for the useful discussions and comments during the work.

References

[1] Aliakbari, M., Geunes, J., and Sullivan, K. M., "The single train shortest route problem in a railyard," *Optimization Letters*, Vol. 15, No. 8, 2021, pp. 2577–2595. https://doi.org/10.1007/s11590-021-01761-w.

[2] FederalRailroadAdministration, "Unmanned Aircraft System Applications in International Railroads," , 2018. URL https://railroads.dot.gov/elibrary/unmanned-aircraft-system-applications-international-railroads, (accessed 04 May 2022).

[3] SNCF, "France: Demonstrating the use of drones for railway maintenance and security," , 2015. URL https://uic.org/com/enews/nr/464/article/france-demonstrating-the-use-of?page=iframe_enews, (accessed 05 May 2022).

[4] Lee, K. S., Ovinis, M., Nagarajan, T., Seulin, R., and Morel, O., "Autonomous patrol and surveillance system using unmanned aerial vehicles," *2015 IEEE 15th International Conference on Environment and Electrical Engineering (EEEIC)*, 2015, pp. 1291–1297. https://doi.org/10.1109/EEEIC.2015.7165356.

[5] Flammini, F., Naddei, R., Pragliola, C., and Smarra, G., "Towards Automated Drone Surveillance in Railways: State-of-the-Art and Future Directions," *Advanced Concepts for Intelligent Vision Systems*, edited by J. Blanc-Talon, C. Distante, W. Philips, D. Popescu, and P. Scheunders, Springer International Publishing, Cham, 2016, pp. 336–348.

[6] Flammini, F., Pragliola, C., and Smarra, G., "Railway infrastructure monitoring by drones," *2016 International Conference on Electrical Systems for Aircraft, Railway, Ship Propulsion and Road Vehicles & International Transportation Electrification Conference (ESARS-ITEC)*, 2016, pp. 1–6. https://doi.org/10.1109/ESARS-ITEC.2016.7841398.

[7] Henrickson, J. V., Rogers, C., Lu, H.-H., Valasek, J., and Shi, Y., "Infrastructure assessment with small unmanned aircraft systems," *2016 International Conference on Unmanned Aircraft Systems (ICUAS)*, 2016, pp. 933–942. https://doi.org/10.1109/ICUAS.2016.7502652.

[8] Lin, J., Wang, Z., Wang, Y., Lin, Y., and Du, X., "Monitoring abandoned dreg fields of high-speed railway construction with UAV remote sensing technology," *International Conference on Intelligent Earth Observing and Applications 2015*, Society of Photo-Optical Instrumentation Engineers (SPIE) Conference Series, Vol. 9808, edited by G. Zhou and C. Kang, 2015, p. 980808. https://doi.org/10.1117/12.2207421.

[9] Nintanavongsa, P., Yaemvachi, W., and Pitimon, I., "Performance Analysis of Perimeter Surveillance Unmanned Aerial Vehicles," *2019 7th International Electrical Engineering Congress (iEECON)*, 2019, pp. 1–4. https://doi.org/10.1109/iEECON45304.2019.8938883.

[10] Nigam, N., and Kroo, I., "Persistent Surveillance Using Multiple Unmanned Air Vehicles," *2008 IEEE Aerospace Conference*, 2008, pp. 1–14. https://doi.org/10.1109/AERO.2008.4526242.

[11] Jung, S., Jo, Y., and Kim, Y.-J., "Aerial Surveillance with Low-Altitude Long-Endurance Tethered Multirotor UAVs Using Photovoltaic Power Management System," *Energies*, Vol. 12, No. 7, 2019. https://doi.org/10.3390/en12071323, URL https://www.mdpi.com/1996-1073/12/7/1323.

[12] Xu, J., Chen, Y., and Xiong, L., "Multi-UAV Mission Planning for Fuel-constrained Persistent Surveillance Problem," *2020 10th Institute of Electrical and Electronics Engineers International Conference on Cyber Technology in Automation, Control, and Intelligent Systems (CYBER)*, 2020, pp. 203–208. https://doi.org/10.1109/CYBER50695.2020.9279163.

[13] Cho, J., Sung, J., Yoon, J., and Lee, H., "Towards Persistent Surveillance and Reconnaissance Using a Connected Swarm of Multiple UAVs," *IEEE Access*, Vol. 8, 2020, pp. 157906–157917. https://doi.org/10.1109/ACCESS.2020.3019963.

[14] Karydis, K., and Kumar, V., "Energetics in robotic flight at small scales," *Interface Focus*, Vol. 7, No. 1, 2017. https://doi.org/10.1098/RSFS.2016.0088.

[15] Gatti, M., "Complete Preliminary Design Methodology for Electric Multirotor," *Journal of Aerospace Engineering*, Vol. 30, 2017. https://doi.org/10.1061/(ASCE)AS.1943-5525.0000752.

[16] Biczyski, M., Sehab, R., Whidborne, J., Krebs, G., and Luk, P., "Multirotor Sizing Methodology with Flight Time Estimation," *Journal of Advanced Transportation*, Vol. 2020, 2020, pp. 1–14. https://doi.org/10.1155/2020/9689604.

[17] NVIDIA, "Jetson Nano Developer Kit | NVIDIA Developer," , 2022. URL https://developer.nvidia.com/embedded/jetson-nano-developer-kit, (accessed 09 Aug 2022).

[18] Bauersfeld, L., and Scaramuzza, D., "Range, Endurance, and Optimal Speed Estimates for Multicopters," *IEEE Robotics and Automation Letters*, Vol. 7, 2021, pp. 2953–2960. https://doi.org/10.48550/arxiv.2109.04741, URL https://arxiv.org/abs/2109.04741v2.

[19] Hwang, M.-h., Cha, H.-R., and Jung, S. Y., "Practical Endurance Estimation for Minimizing Energy Consumption of Multirotor Unmanned Aerial Vehicles," *Energies*, Vol. 11, No. 9, 2018. https://doi.org/10.3390/en11092221, URL https://www.mdpi.com/1996-1073/11/9/2221.